Next Steps for Determining the Fine Structure Constant with Bose-Einstein Condensate Interferometry

Eric Cooper,* Daniel Gochnauer, Ben Plotkin-Swing, Katie McAlpine, and Subhadeep Gupta
Physics Department, University of Washington
Seattle, WA 98105
(Dated: September 16, 2017)

This paper describes progress towards the goal of measuring the fine structure constant to an uncertainty of 0.1 ppb with a ytterbium BEC contrast interferometer. The current experimental setup, based on horizontal diffraction beams, is limited by the short (10 ms) freefall time available for atomic manipulation and interrogation. Two broad options for moving forward are adding an initial launch and continuing to optimize the current horizontal setup, or switching to vertical diffraction beams. This paper finds that optimizations within the horizontal setup are likely limited to 1 ppb accuracy, while 0.1 ppb precision is plausible if a vertical geometry is adopted. Switching to the vertical geometry entails new challenges, particularly due to the need to compensate for Doppler shifts due to the gravitational acceleration of atoms. Progress this summer towards compensating for these Dopplar shifts with a digital frequency synthesizer is presented. Also described are tests and modifications performed to ensure that the experiment's time standard is accurate to the level required for precision measurement. Overall, switching to a vertical geometry appears to be a promising way to achieve sub-ppb level accuracy in α and progress has been made this summer to prepare for the transition to the new configuration.

I. INTRODUCTION

The Fine Structure Constant relates the charge of the electron to planks constant, the permittivity of free space, and the speed of light. The resulting dimensionless ratio parameterizes the coupling between light and matter and this constant is both an important parameter for relativistic effects in atomic physics and an important parameter for perturbations in Quantum Electrodynamics. Currently, the most precise measurements of the fine structure constant are made possible due to the fine structure constant's key role in QED calculations of the anomalous magnetic moment of the electron $(g-2)$. Using tenth order Feynman diagrams from QED, $g-2$ may be calculated as a function of α. Assuming the validity of these QED calculations, the most recent measurements of $g-2$, performed by the Gabrielese group at Harvard, produce a value of α with an uncertainty of 0.25 pbb [1,2].

The best measurements of the fine structure constant that do not depend on QED are atomic recoil measurements. The most precise measurement to date was performed by the Biraben group in France, who used cold atoms to achieve a precision measurement of α with an uncertainty of 0.7 ppb [3]. The comparison of this atomic recoil measurement of α to the value implied by the Harvard $g-2$ experiment constitutes the most precise validation of QED to date. As the comparison is currently limited by atomic recoil measurements, improving the sensitivity of a direct measurement of α will immediately improve the level of this comparison. This improved comparison incorporate the effects of muonic and hadronic terms in $g-2$ calculations, opening up further tests for fundamental QED [3,7].

The Gupta interferometry group is one of several groups worldwide that are working to improve the sensitivity of atomic recoil measurements. By using Bose-Einstein Condensates instead of thermal atoms, the Gupta group is able to achieve extended coherence times and produce a working contrast interferometer [4]. This paper will describe the next steps necessary to produce a 0.1 ppb level measurement of the atomic recoil frequency using these contrast interferometers and progress made towards this goal over the course of my REU.

II. MANY-RECOIL CONTRAST INTERFEROMETRY

The Gupta group uses a contrast interferometer, as shown in Figure 1, to precisely measure the recoil frequency of ytterbium. The contrast interferometer works by giving precise momentum kicks to the right and left beams so that they acquire kinetic energy with respect to the central beam. This kinetic energy manifests itself as a frequency shift between the phase evolution rate of the external paths and the central path of the interferometer. By interfering these paths together at the end, the two higher energy paths create a standing wave that beats against the central path creating a fringe pattern that oscillates in time. The phase of this fringe pattern may be varied by changing the total interferometer time and the resulting change in phase is directly proportional to the atomic recoil frequency $\omega_{rec} = \hbar k^2/2m_{Yb}$.

Precise measurements of this recoil frequency, combined with measurements of the mass of ytterbium and the frequency of the applied light, produce a precise measurement for $\hbar$. This measurement of $\hbar$ can be applied to

* Also at Physics Department, Pomona College.; eric.cooper@pomona.edu

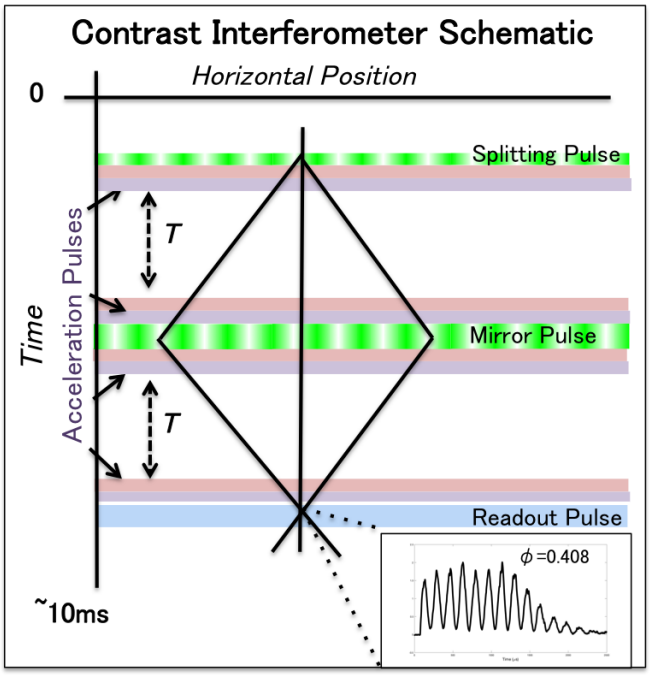

FIG. 1. Schematic describing the manipulation of atoms in a horizontal contrast interferometer. A short pulse in the kaptisa-dirac regime splits the condensate into three arms. The outer two arms are reflected back towards the center and create an interference pattern, from which the atoms' phase can be read. In order to maximize the total phase evolution, each arm is accelerated and decelerated during the spaces between the splitting, mirror and readout pulses. Separately applied third order Bragg pulses are used to preform the accelerations.

the following expression for the fine structure constant.

$$\alpha^2 = 8\pi \frac{R_\infty}{c} \frac{m_{Yb}}{m_e} \frac{\omega_{rec}}{k^2} \tag{1}$$

The Rydberg constant is known to 5×10^{-12} from hydrogen spectroscopy measurements, and the speed of light is defined in SI units [5]. Thus the first term in this expression is far from the limiting factor in determinations of α. The ratio of the mass of ytterbium to the mass of an electron is known at the 0.1 ppb level from measurements with Penning traps [6]. The goal for atomic recoil measurements is to measure the final term to a level of sensitivity comparable to that of the mass measurements. Combined with the current levels of sensitivity in the Rydberg constant and the ytterbium mass, a measurement of the recoil frequency at the 0.1 ppb level can reduce the total uncertainty in α to 0.07 ppb.

A. Phase Evolution in a Contrast Interferometer

The total uncertainty in recoil measurement in a contrast interferometer can be divided into uncertainty in phase measurements and uncertainty in timing measurements.

$$\omega_{rec} = \frac{\partial \phi}{\partial T} \Rightarrow \left(\frac{\Delta \omega_{rec}}{\omega_{rec}}\right)^2 = \left(\frac{\Delta \phi}{\phi}\right)^2 + \left(\frac{\Delta T}{T}\right)^2 \tag{2}$$

The total uncertainty in phase has been fixed in recent experiments at approximately 10 mrad. Although recent developments in laboratory (not discussed in detail in this report) suggest that sensitivity beyond this level may be possible, it remains a good benchmark for understanding the sensitivity in phase. Thus in order to reach 0.1 pbb in ϕ, the total phase accumulation must be on the order of 100 million radians or absolute resolution must be further improved. Similarly, the time T must be measured to within 0.1 ppb, which is equivalent to either 1 ps precision out of a total free evolution time of 10 ms or 10 ps precision out of a total free evolution time of 100 ms. Timing devices that can measure at both levels of precision exist, but it requires care to ensure that the timings relevant to the experiment are measured this precisely.

For a interferometer with a momentum separation between the central path and each arm of one photon recoil (N = 1), and a maximum free evolution time of 10 ms, the total phase accumulation is 930 radians, which corresponds to 11 ppm, 5 orders of magnitude above the eventual desired sensitivity. The route that the Gupta interferometry group has taken to further increase the sensitivity of recoil measurements is to increase the rate of phase evolution by increasing the energy separation between two paths. To do this, momentum kicks are added to each of the side arms in Figure 1. This added momentum increases the rate of phase evolution in proportion to the added kinetic energy, which is the square of the number of momentum kicks. The total resulting phase evolution is given by the equation,

$$\phi = \omega_{rec}(2N)^2(2T), \tag{3}$$

where N is the number of photon pairs that each branch interacts with and T is the total free evolution time in each gap between acceleration and deceleration pulses.

The Gupta group has successfully increased the number of photon recoils up N = 28. However, accelerating the atoms with such a large number of photon recoils requires a large fraction of the total time available before the atoms fall out of the beam. Due to the time needed for the acceleration of the atoms, the total amount of time remaining for free evolution is only about 2 ms and the total phase evolution is only able to be increased to approximately 120,000 radians in the current configuration. Due to limitations in the amount of time that can be spent within the diffraction beams before the atoms fall out, further increasing the number of photon recoils at this stage would not further increase the total phase evolution. To increase this total phase evolution, adjustments to the experiment must be made that will increase the total time within the diffraction beams, allowing both for improved free evolution time and potentially addi-

tional acceleration pulses to achieve even higher momentum separations.

III. ANALYZING GEOMETRIES FOR A FUTURE INTERFEROMETER

For the next steps towards achieving 0.1 ppb sensitivity with a contrast interferometer, the total amount of time available to manipulate and allow the atoms to freely evolve must be increased. Broadly, there are two ways to attempt to achieve this: remain with horizontal diffraction geometry and use various tricks to increase phase evolution, or switch to a vertical diffraction geometry and partially redesign the experiment so that the atoms are manipulated with light in the same direction as that which they are falling. The primary advantage of the horizontal configuration is that it is currently set up, tested and working, albeit at a sensitivity 2-3 orders of magnitude bellow the ultimate goal. The enticement of a vertical geometry is primarily that the 10 cm vertical height of the vacuum chamber offers substantially more space than the 0.5 mm of workable space within the current diffraction beam. This section discusses in detail the constraints associated with each geometry.

A. Horizontal Diffraction Beams

Within the horizontal geometry, the primary constraint is the amount of time before atoms fall out of the uniform portion of the Gaussian beams and become no longer manipulable with light. In the current geometry, this workable distance is 0.5 mm, corresponding to a freefall time of 10 ms. This time, $T_{tot} = 10$ ms must be shared between acceleration and free evolution time. Thus the total free evolution time, $2T$ is constrained by the amount of time needed for the acceleration pulses (t_{acc} per $3N$) plus the amount of time needed to operate the diffraction pulses of the base $N = 1$ interferometer.

$$T_{tot} = 2T + t_{N=1} + t_{acc}\left(\frac{N-1}{3}\right) \tag{4}$$

Rearranging the expression with the assumption that $t_{N=1} - t_{acc}/3 << T_{tot}$ we can obtain a simpler expression for T that we can then substitute into the expression for total phase

$$T = \frac{T_{tot}}{2} - t_{acc}\frac{N}{6} \tag{5}$$

The total phase evolution in this case is

$$\phi = \omega_{rec}(2N)^2\left(T_{tot} - t_{acc}\frac{N}{3}\right) \tag{6}$$

The expression for phase is maximized when additional gains from the N^2 term in phase evolution are canceled out by loss of free evolution time due to the acceleration pulses. This maximum may be found by setting the derivative with respect to N equal to zero.

$$0 = 8\omega_{rec}NT_{tot} - 4\omega_{rec}N^2t_{acc} \tag{7}$$

$$N = \frac{2T_{tot}}{t_{acc}} \tag{8}$$

Thus the maximum phase evolution always occurs in this configuration when the total time spent accelerating, $\frac{N}{3}t_{acc}$ is 2/3 of the total available time. For the current experimental parameters, $t_{acc} = 1020$ µs and $t_{tot} = 10$ ms, the maximum possible phase evolution (rounded to nearest accessible value) occurs at $N = 19$. The corresponding free evolution time and phase evolution are $T = 1.8$ ms and $\phi = 120000$ rad, consistent with the current limitations. To increase phase evolution beyond these current values, either the total amount of time within the beam must be increased or the acceleration times must be decreased. Within the constraints inherent to a horizontal diffraction geometry, the principal options for improving t_{acc} and T_{tot} are introducing a vertical launch, introducing simultaneous Bragg pulses for the left and right arms, and using Bloch oscillations to increase the acceleration rate. The following paragraphs describe each of these options in detail.

1. Vertical Launch

Adding a vertical launch increases the total amount of interferometer time by a factor of 2 by allowing the experiment to take advantage of freefall time on the way up in addition to freefall time on the way down. By increasing the total amount of time available for the experiment from 10 ms to 20 ms, both the optimal number of acceleration pulses and the total amount of time left for free evolution approximately double. The new values of $N = 40$ and $T = 3.2$ lead to a total phase evolution of $\phi = 960000$ rad. This is an improvement by a factor of 8, though it is important to note that such an improvement depends on successfully achieving readable signals from $N = 40$ data sets. This would require further improvements in Bragg pulse efficiency as $N = 28$ signals are currently close to the limit of producing a readable signal. If the total number of acceleration pulses remained at $N = 28$, the free evolution time available would be $T = 5.2$ ms and the total phase would be $\phi = 760000$ rad, slightly more than six times better than the current maximum phase evolution.

2. Simultaneous Bragg Pulses

In the current design, each arm of the interferometer is accelerated separately by Bragg acceleration pulses. A Bragg acceleration pulse is a pair of beams detuned by $\pm\delta$ from their average frequency of f_0. Due to Doppler

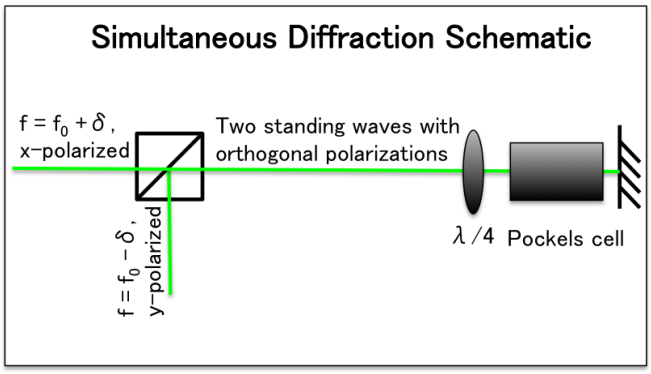

FIG. 2. Two perpendicular beams with opposite detunings, δ, come together on beam cube. The pair of beams travel across the chamber and then are reflected back, passing through a $\lambda/4$ plate twice and in the process exchanging polarizations. The 4 beams come together to form two standing waves with orthogonal polarizations. Since in the case where $\delta = 0$, the two standing waves can interfere with each other, a Pockels cell is added to selectively cancel the effects of the $\lambda/4$ plate in this scenario.

effects, these two beams form a standing wave in a frame traveling at a velocity of $v = \delta\lambda$ with respect to the lab frame. This moving standing wave is able to accelerate atoms in much the same way a tennis racket accelerates a tennis ball, with reflections when viewed from the frame of the standing wave (or tennis racket). Atoms Bragg reflect off of the moving wave and gain momentum with respect to the lab frame by absorbing and re-emitting several photons. The effect is substantially stronger for transitions involving fewer photons, so it is possible for these waves to interact nearly exclusively with the outer arms of the interferometer. To do this, standing waves are created alternatively in frames with velocities close to those in each of the outer arms, but not close enough to the lab frame to substantially disturb atoms in the center path of the interferometer.

An option to increase the rate at which momentum can be transferred to the atoms is to use a pair of standing waves (in opposite moving frames) with perpendicular polarizations to accelerate the right and left interferometer arms of atom simultaneously. The Bragg acceleration pulses used in the current design unfortunately a single polarization of light to produce a standing wave in a frame moving at velocity of v to the lab frame. In contrast to the current use of sequential acceleration pulses, both polarization options are used simultaneously produce both the $+v$ and $-v$ standing waves. A schematic of how this may be realized in practice can be seen in Figure 2.A Pockels cell is necessary to cancel out the quarter wave plate in the the case of a standing wave pulse ($v = 0$). If the Pockels cell were not present, the two perpendicular polarization standing waves would interfere with each other, as their phase relationship is not fixed. With small vibrations in the mirrors and optics, the two waves are liable to move into configurations that cancel out the periodic stark shift potential that is key to the standing waves' ability to manipulate the atoms. By using the Pockels cell to cancel the quarter waveplate, only a single standing wave can be used, thus avoiding this complication.

3. Bloch Oscillations

A further option to increase the rate of momentum transfer to the atoms is Bloch oscillations. Bloch oscillations permit an increased acceleration rate by transferring many pairs of photons to the atoms in a coherent process. Instead of using constant velocity standing waves of light for 2-3 photon pair transfers, Bloch oscillations use accelerating standing waves of light that pull the atoms along with them by transferring the momentum from as many pairs of light as is necessary. These oscillations are both faster and more efficient than the Bragg pulses that are currently used to accelerate the two arms of the interferometer. Although it takes a fair amount of time to turn on lattices used for Bloch oscillations, once the lattice is on, it can be used for an arbitrarily long time acceleration runs. The use of Bloch oscillations has not yet been successfully implemented in the Gupta laboratory to produce a precision ytterbium contrast interferometer, but the higher efficiencies as compared to Bragg pulses could permit exceptionally large momentum transfers, perhaps as large as 50 photon pairs instead of the current maximum of 28 photon pairs.

A challenge with the use of Bloch oscillations for an interferometer however, is that in order to take advantage of the increased acceleration times, all units of momentum transfer must be done at the same time within a single arm. Thus in a simple situation where one side is accelerated first and then the second side is accelerated, a substantial amount of time elapses, during which vibrations can change the orientation of the beam.

A further challenge with Bloch oscillations is that they cause substantial diffraction phases, undesired phase evolution due direct interactions between the atoms and light. With the quality of intensity stabilization currently available to the experiment, the total diffraction phase is large enough to completely wash out the final interferometer signal, at least in the case of sequential accelerations of the two arms. This and the challenges due to the sequential accelerations of the two arms led the lab to abandon a prior effort to use Bloch oscillations to accelerate the arms of the interferometer.

One option available to break new ground with the use of Bloch oscillations in the interferometer is apply the same double standing-wave arrangement shown in figure 2 with Bloch oscillations. These simultaneous Bloch oscillations would control against system vibrations that would otherwise occur between sequential Bloch accelerations. It also is easier to construct a symmetric, closing interferometer when simultaneous Bloch oscillations are used. If intensity stabilization is further improved as well,

the Bloch oscillations may prove to be able to produce a closed interferometer with a consistent phase.

4. *Prognosis for Horizontal Sensitivity*

If all three proposed changes to the horizontal geometry were implemented, the experiment would dramatically improve its sensitivity, but would still be hard-pressed to reach the level of sensitivity needed for a 0.1 ppb level measurement of α.

With the addition of a vertical launch, the total amount of time available would increase to 20 ms. With the addition of Bloch oscillations conducted simultaneously in each beam the rate of momentum transfer could optimistically be increased such that accelerating to N = 50 would be achievable in relatively small portion of the 20 ms flight time. In the most optimistic scenario, where the acceleration times are negligible and thus $2T = 20$ms, the total phase evolution would be,

$$\phi = \omega_{rec}(2N)^2(2T) = 4.7 \times 10^6 \text{ rad.} \tag{9}$$

For this amount of phase evolution, 0.1 ppb relative precision would require an absolution precision of 0.47 mrad, twenty times lower than the current precision. If the precision of phase readout remains at the current level of 10 mrad, the horizontal precision would reduce to 2 ppb. The corresponding 1 ppb precision in α in this case would start to become competitive with measurements done in rubidium [3]. However, as this scenario is already very optimistic, it is hard to see a horizontal geometry based on the current setup achieve levels of precision at the desired 0.1 ppb level.

B. Vertical Diffraction Beams

A second option for increasing the total amount of time available for phase evolution is transforming the experiment into an entirely vertical geometry. By using vertical diffraction beams, the total amount time available increases from the freefall time within a 0.5 mm beam to the freefall time within a 10 cm vacuum chamber. This allows for dramatic improvements in both free evolution time and acceleration time.

A interferometer within a vertical geometry can be realized using a method like that shown in Figure 3. After falling most of the way to the bottom of the chamber, the BEC is given a launch with Bloch oscillations to maximize its freefall time within the chamber. During freefall, the same splitting, acceleration and mirror pulses from the horizontal contrast interferometer are applied. All of these pulses are chirped in order to compensate for the effects of gravity. The benefits of this increased freefall time are described and quantified in this section.

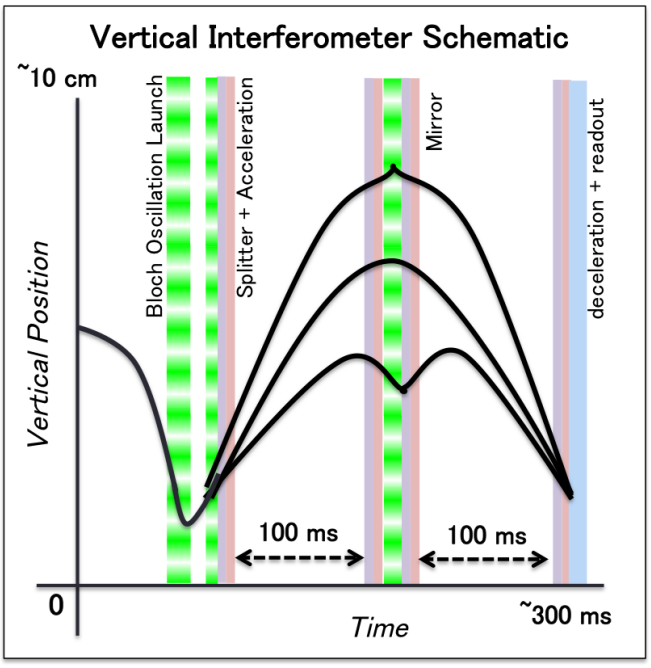

FIG. 3. Schematic for the atomic beam paths within a vertical interferometer. The schematic is broadly the same as a horizontal contrast interferometer with splitting, acceleration, mirror and readout pulses. These pulses are chirped in order to compensate for the effects of gravity. The primary addition to the pulses from the horizontal interferometer is a large initial launch, realized with Bloch oscillations, that allows the experiment to take advantage of freefall within the entire chamber.

1. *Maximizing Phase Evolution*

In the case of the vertical geometry, the primary constraint is the size of the vertical chamber. In contrast to the horizontal setup, the total amount of time spent on acceleration pulses is negligible. Instead, the primary modification from simply setting the free evolution time to the free fall time is due to the need to account for the separation of top and bottom arms of the interferometer from the freefall path that the center arm follows. The initial interferometer splitting pulse adds a relative velocity of $2Nv_{\hbar k}$ where $v_{\hbar k} = 4$ mm/s is the single photon recoil velocity of ytterbium. This means that the total amount of time for the atoms to fall from the top of the vacuum chamber to the bottom of the vacuum chamber is given by the solution to the equation of motion under gravity with initial velocity $2Nv_{\hbar k}$ and total usable chamber size of $d = 7$cm (reduced from 10 cm to avoid contact with the walls). This is expressed algebraically as

$$d = \frac{1}{2}gT^2 + 2Nv_{\hbar k}T \tag{10}$$

$$T = \frac{-2Nv_{\hbar k} + \sqrt{(2Nv_{\hbar k})^2 + 2gd}}{g} \tag{11}$$

Using this expression for time, it is possible to once again compute the total phase evolution as a function of the number of recoils, given below.

$$\phi = \omega_{rec}(2N)^2(2T) \tag{12}$$

$$\phi = 8\omega_{rec}N^2\left(\frac{-2Nv_{\hbar k} + \sqrt{(2Nv_{\hbar k})^2 + 2gd}}{g}\right) \tag{13}$$

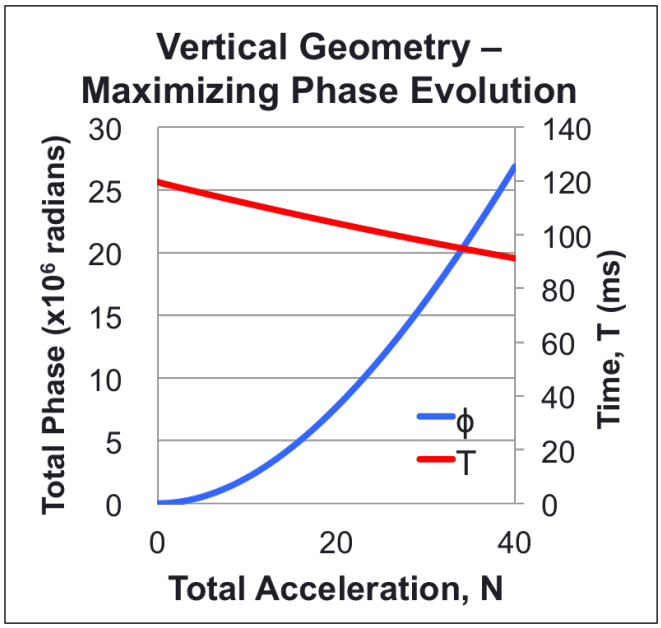

FIG. 4. Free evolution time and phase evolution as a function of the number of photon recoils, N. As acceleration is increased, the time available for free evolution decreases slightly, but the N^2 dependence in the phase means that the maximum free evolution increases without bound for all reasonable values of N.

This expression for phase evolution and the expression for time are plotted in Figure 4. Since, in the limit of large N, the total time decays like $1/N$, while the phase grows like N^2T, the total amount of phase evolution is not bounded by the constraints taken into account by this model. In practice, the limiting factor is likely to be the decreasing number of atoms remaining to contribute to the diffraction grating after the a large number of diffraction pulses. From experiments in the current horizontal geometry, it appears that at N = 25, the interferometer signal can still be seen if multiple runs are averaged together. Further increases in N are likely possible, but as increasing the total interferometer time will also impact the visibility of the interferometer it is risky to assume dramatic improvements beyond the current N = 25 setup are easily feasible. Even if no further improvements in N are made however, the total phase evolution permitted by the vertical geometry is a dramatic improvement over the current horizontal setup. Substituting in N = 25 in the new equations for maximized phase yields

$$T = \frac{-2Nv_{\hbar k} + \sqrt{(2Nv_{\hbar k})^2 + 2gd}}{g} = 100 \text{ ms} \tag{14}$$

$$\phi = 8\omega_{rec}N^2\,(100 \text{ ms}) = 12 \times 10^6 \text{ rad} \tag{15}$$

Even in this conservative scenario, assuming no further improvements to the amount of acceleration, the total phase evolution in the vertical geometry is one hundred times larger than the current horizontal setup. It is also twice that of the best case scenario for improvements in which and initial vertical launch is installed and Bloch oscillation are implemented and achieve $N = 50$ in a negligible fraction of 20 ms. Further, the vertical scenario permits a free evolution time of 2T = 200 ms, ten times larger that the next best scenario with vertical launch. This permits dramatically more straightforward measurements of timing precision at the 0.1 ppb level as instead of the 2 ps timing precision required in the vertical case, it requires 20 ps timing precision, which can be achieved by averaging multiple runs of a time-to-digital converter.

2. *New Challenges*

Switching to a vertical scenario introduces new technical challenges. First, since the atoms are now in freefall within the same dimension as the diffraction beams, the standing waves used to Bragg diffract the atom must be constantly tuned so that they remain standing waves within the correct reference frame with respect to the atoms. Second, since the current blue readout light mechanism requires the use of specific view ports in order for light to reflect off the atoms at the Bragg angle, switching to the vertical geometry will require a redesign of the readout light. Third, many of the systematic effects, as enumerated in Alan Jamison's thesis [6] scale like T^2 and thus need to be reconsidered as the total interferometer time is increased by a factor of ten. In particular, effects due to gravity, stray electric fields and the rotation of the earth need to be taken into new consideration as they may no longer be negligible.

The technical challenge of creating standing waves that chirp to match the Doppler shift due to gravity can be met by using a direct digital synthesizer to match the frequency shifts due to gravity. As long as the local acceleration of gravity is known with sufficient precision, an applied frequency difference between the two beams, 2δ, that sweeps with rate $\dot{\delta} = \frac{g}{\lambda}$, will create standing waves that are tuned to match the velocity of the atoms. Since matching the sweep rate is important primarily for the efficiency of the Bragg pulses rather than for the overall accuracy of the experiment, uncertainties in the magnitude of the local gravitational field can ultimately be accounted for by tuning the sweep rate for maximal efficiencies. A more detailed description of how to implement these frequency sweeps is given in section IV.

The current system uses blue light, which is reflected off of the density grating produced by the atoms. Since the atomic grating spacing is fixed by the green light used for the diffraction beams, the angle of Bragg reflection with blue light is fixed at approximately 45 degrees. Within the current setup with horizontal diffraction beams, this reflection is optimal to enter and exit through two view ports situated to the sides of the horizontal diffraction beam. Unfortunately, no analogous viewports exist at 45 degrees with respect to a vertical beam direction. This leaves three options: utilize the large bottom viewport for both the vertical diffraction beams and the readout, switch back to green readout light, or redesign the vacuum chamber to have additional optical access.

The first option of utilizing the bottom viewport for both the vertical diffraction beams and for readout is complicated by the magnetic coils wrapped around the viewport. These coils require the readout beams, which enter at 45 degree angles, to pass about 2 cm above the glass at the edge of viewport. This means that for optical access with the readout beams, the atoms must essentially be flush with the glass at the end of the experiment. This leads to undesirable electrostatic effects. Switching to green readout light would increase the Bragg reflection angle to 90 degrees, and allow use of the same optical axis as the diffraction beam. This leads to more worry about backscattering noise, but is far more feasible with the current geometry of the vacuum setup. The final option of redesigning a portion of the vacuum system would allow for blue readout to be re-instated without the need for the atoms to closely approach the edges of the chamber. A resigned vacuum system could also have the additional advantage of further increasing the available freefall distance with, for instance, a vertical tube added above the current chamber. The downside to this option is the substantial time commitment required to break vacuum and the risk of damaging the currently functioning setup in the process of redesigning the chamber. In the near future, the use of green readout light again is likely the most feasible solution.

The systematic effects due to gravitational gradients, the Earth's rotation and stray electric fields are a greater concern for the overall accuracy of the experiment. The total systematic shift due to the earth's rotation $\Delta\phi_R/\phi$, gravitational gradients $\Delta\phi_g/\phi$, and stray electric fields $\Delta\phi_E/\phi$ are calculated by Adam Jamison in his thesis on pg. 113-118 [7]. The numerical values from the thesis assume the horizontal geometries parameters of the old setup, $T = 10$ ms, $t_{acc} = 1$ ms, $d = 5$ cm , $q = 76$ pC and Seattle's latitude of 47 degrees.

$$\Delta\phi_R/\phi = \left(\frac{2\pi T}{8.6410^4\text{s}}\right)^2 \cos(47^\circ) = 2.5\times10^{-9} \quad (16)$$

$$\Delta\phi_g/\phi = \frac{\partial g_x}{\partial x}(\frac{1}{3}T^2 + t_{acc} * T) = -1.2\times10^{-10} \quad (17)$$

$$\Delta\phi_E/\phi = 10\frac{p}{m}\frac{k^2q^2}{d^6}(\frac{1}{3}T^2 + t_{acc} * T) = 1\times10^{-10} \quad (18)$$

All of these effects grow as T^2, so the ten-fold increased time from the time assumed in Alan Jamison's thesis to the times possible in the vertical geometry cause these effects to grow by a factor of 100. Thus effects that were almost negligible in the case of the horizontal configuration must be taken into consideration. In the case of the rotation of the earth and gradients in the local gravitational field, the total size of the effect cannot be changed, but with calculations of the effect of earth's rotation to within 4×10^{-4} and gravity gradients to within 1×10^{-2}, the remaining uncertainty can be reduced to below 0.1 ppb.

The case of electric charge on the viewports is more concerning, as the effect grows like the distance to the veiwport to the sixth power in addition to growing as T^2. To avoid this term growing ridiculously large, the atoms must be kept a safe distance from the sides of the container. The size of 7 cm used for calculations earlier in this paper would leave approximately 1.5 cm of clearance to the view ports, one third of the 5cm assumed by Alan Jamison's calculations. Thus for the same charge on the viewports, the systematic effect is expected to grow by $3^6\times10^2 = 73,000$. With a $q = 76$ pC charge, the maximum amount of acceptable charge from the horizontal configuration, this effect would be 7.3 ppm, far beyond the acceptable limits.

Luckily, the effect also grows proportional to the square of the source charges, so reducing the amount of charge on the viewports is an effective way to reduce the scale of this effect. In order to reduce the effect down to below the 0.1 ppb sensitivity threshold, the charge on the viewport must be now to be less than 76 pC$/\sqrt{73000} = 280$ fC. It should be possible to measure charge accumulations to this level of sensitivity if needed as charge measurement devices can measure values as low as 1 fC. However, it will no longer be possible to assume, as is done with the current experiment, that any relevant charge accumulation is so large that confetti would be sticking to the viewports if there were a problem [7] (footnote pg. 118). It is also possible to sacrifice some vertical space in order to further increase the 1.5 cm buffer cited here.

3. *Outlook for Vertical Sensitivity*

Overall, vertical diffraction geometry promises dramatically higher sensitivity than the current horizontal configuration. The increase to a total phase evolution of 1.2×10^7 rad from the current 1.2×10^5 rad would increase the sensitivity a priori by a factor of 100 from 8×10^{-8} to 8×10^{-10}. This approaches the desired sensitivity and if the the absolute phase uncertainty is further reduced from 10 mrad down to 1.2 mrad (equivalent to the $1/\sqrt{N}$ shot noise for 7×10^5 photons), it will be possible to achieve the goal of 1×10^{-10}. Also, the required timing precision will be reduced to 200 ms $\times\, 10^{-10} = 20$ ps

from the 1-2 ps needed for the horizontal configuration. This is substantially easier to accomplish with the run-to-run timing stability of outputs of Cicero is 1 ns. An uncertainty in the mean of 20 ps can be achieved with statistical averaging of 2500 runs (10 hrs at 15 s per run) rather than 250000 runs needed for 1 ns$/\sqrt{N} = 2$ ps (100 days at 10hrs per day). From the standpoint of precision timing and precision measurements of phase, the vertical geometry is superior to even the most sophisticated adjustment we expect to be able to make to the horizontal configuration.

IV. ADDRESSING TECHNICAL CHALLENGES FOR VERTICAL GEOMETRY

In addition to analyzing to the benefits and drawbacks of switching to a vertical geometry as compared to maintaining the current horizontal geometry, I began work on the additional equipment needed for a transition into the vertical configuration, particularly the direct digital synthesizer used to chirp vertical beams. I also used the same measurement device that I employed to test my DDS box to test the timing accuracy of the current experiment and discovered timing issues in both the Cicero word generator guiding the experimental timing and the quartz clock that had previously been used as the timing standard for the experiment.

A. Building a DDS

For either adding a vertical launch to a primarily horizontal diffraction setup or switching to an entirely vertical diffraction setup, it is necessary to have a new frequency generator to control the Acousto-optic modulators (AOM) which manipulate vertical beams. For a vertical launch with Bloch oscillations, an additional DDS is needed to make the frequency sweep for a Bloch oscillations launch. For a fully vertical diffraction setup, the additional DDS is needed to make the frequency sweep for Bloch oscillations and to compensate for gravity during diffraction by chirping the beams.

1. Construction of DDS driver for AOM

Controlling an AOM requires precisely controlled radio frequency signals (typically about 200 MHz) that are amplified to have enough power to effectively drive the piezo in the AOM (on the order of several hundred mW). The signal generator that was built for the vertical beam has three primary components in the RF path: a direct digital synthesizer, a variable gain amplifier and a fixed gain amplifier. The direct digital synthesizer is the core of the design and produces precise frequency sweeps necessary to chirp the diffraction beams. The parameters of these sweeps are set using serial inputs provided by an Ardunio also stationed within the control box. An input 10 MHz clock signal provides the reference signal for precise calibration of frequencies that are produced. The final output frequency can be controlled to one part in 2^{32} out of 1 GHz = 0.23 Hz with timing steps of as little as 4 ns. By picking both the width and height of each step in a frequency sweep appropriately, the rate of the frequency sweep can be precisely tuned. This permits smooth frequency sweeps that can compensate for the Doppler shift associated with the acceleration from gravity.

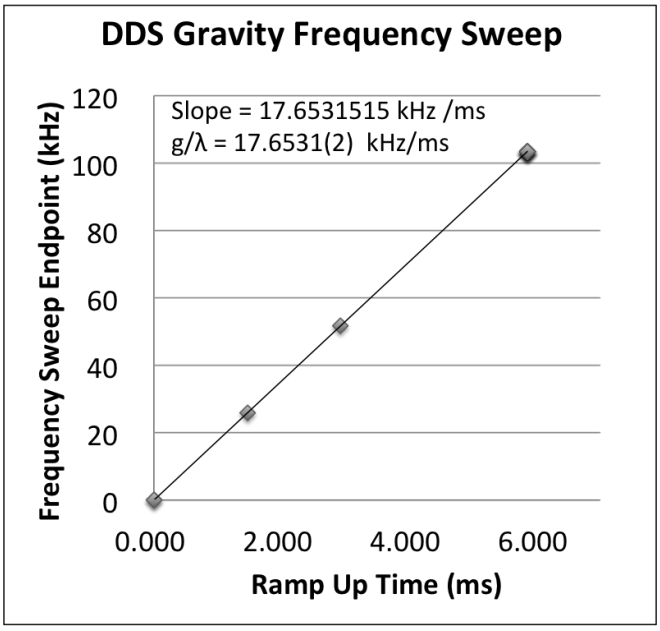

FIG. 5. Results of a test of the DDS frequency sweep. The nominal value for the range of the frequency sweeps (confirmed with a frequency counter) is plotted on the y-axis. The time of the ramp measured directly from the DDS DR_OVR pin is plotted on the x-axis. Each point is the average of several hundred measurements and has an uncertainty of approximately 3 ps. The corresponding uncertainty 0.5 ppb, far larger than the uncertainty in the local gravitational field.

To confirm that the DDS was functioning and producing frequency sweeps with the expected level of precision, we both checked the output frequencies of the devices with a frequency counter and measured the rate of the frequency sweep by monitoring the digital ramp over (DR_OVR) output pin on the DDS. The output frequencies as tested by a frequency counter were exactly as expected to within the 1 ppm accuracy of the frequency counter. The actual values are likely substantially more precise since it is digitally linked to a high fidelity cesium frequency source. We checked the rate of frequency ramps by measuring the amount of time that the DR_OVR pin was low for a variety of nominal frequency sweeps. Plotting these times against the nominal magnitude of the frequency sweeps gives a line where the slope is the programmed compensation for the Doppler shift due to gravity. As shown in Figure 5 the slope con-

firmed that the DDS device is able to produce the desired $\dot{\delta} = 17.6531(2)$ MHz frequency shift to a level of precision limited by knowledge of the local gravitational field rather than by the DDS itself. The value for the local gravitational field was calculated from the USGS 2008 model via the Wolfram Alpha Knowledgebase. After the experiment is running, this sweep rate may be tuned to the appropriate value to maximize the efficiency of all acceleration pulses [8].

With a functioning DDS at the core of the signal generator, the two amplifiers provide control over the amplitude of the signals sent to the AOM. This control is necessary to feed back on the amplitude of the diffraction beams so that the intensity of the light at the atoms is well controlled. This control circuit could not be tested fully without incorporating the DDS box into the experiment and testing it directly on an AOM, but preliminary tests showed that we could achieve a strong signal with an appropriate and controllable power output. The combination of the tests on the DDS and the amplification circuit suggest that the device is complete and ready for implementation in the next generation of the experiment.

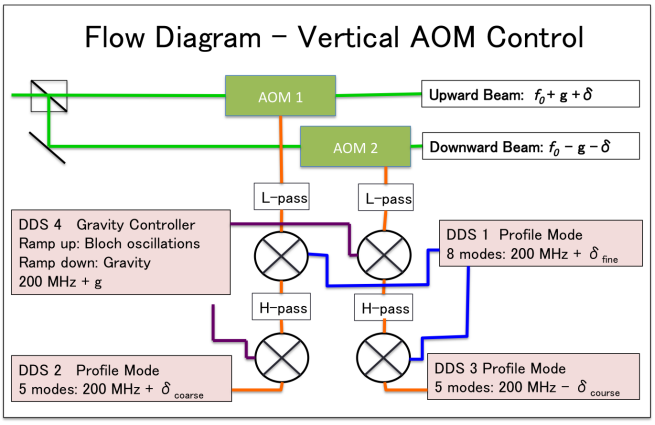

FIG. 6. Schematic describing a proposed control circuit for vertical diffraction beams. The circuit uses direct digital synthesizers to produce signals that create standing waves within the falling reference frame of the atoms. DDS 1-3 produce linear offsets between the beams to control whether the beams are acceleration or mirror pulses. DDS 4 produces a linear frequency sweep that can be used to either produce a sweep for the initial Bloch oscillation launch or to compensate for gravity during the remainder of the experiment. RF multipliers combined with filters add and subtract signals from different synthesizers.

2. *New design for Output Signals*

With the DDS functioning appropriately and producing precise frequency sweeps, I designed a new RF configuration for proposed use in a future vertical configuration. This collection of 4 synthesizers can control the diffraction beams by adding the frequency sweep produced by one DDS to the fixed frequency differences that control whether diffraction beams act as acceleration pulses or mirror pulses. The design shown in figure 6 works to address three major goals of for the new AOM driving system: ensuring that the mean frequency is controlled (so that the momentum kick is constant), adding on the frequency sweep to compensate for gravity, and achieving all of the desired fixed frequency differences needed to split, accelerate and reflect the atoms.

The key addition in this new design as compared with the current setup is the addition of a RF multiplier so that frequencies from more than one DDS can be added together (mixer plus high-pass filter) or subtracted from on another (mixer plus low-pass filter). This means that one DDS can be used to compensate for gravity with a steady frequency sweep while the other three DDS setups can be used to apply the fixed differences that control the type of diffraction.

The use of RF mixers makes it straightforward to keep the mean frequency of the pair of diffraction beams constant. All that is needed is to add the output of a DDS to one beam while subtracting it from the other. By the maintaining this symmetry between the two beams and a constant mean value, the momentum kick from two-photon processes is held constant, eliminating the need for corrections - as are required in the current setup.

Since at least 17 different frequency separations $(0, \pm5, \pm11, \pm17, \pm23, \pm29, \pm35, \pm41, \pm47) * f_{2\hbar k}$ are necessary to produce all of the acceleration pulses used in the $N = 25$, sequence and a single DDS can only produce 8 distinct frequencies, two DDS are added together to yield 64 different frequencies. This is possible if one DDS provides the coarse adjustments and the other provides fine tuning. The correct choice of steps for these course and fine adjustments permits the 4 DDS setup shown in Figure 6 to achieve all of the frequency separations needed for acceleration up to $N = 73$. This is possible if $\delta_{coarse} = [0, 5, -47, 53, -95, 101, -143] * f_{\hbar k}$, and $\delta_{fine} = [0, 1, 2, 3, 4, 5, 6, 7] * 6 * f_{\hbar k}$ where $f_{\hbar k}$ is the frequency of the Doppler shift needed (in each beam) to produce a standing wave in a frame moving with the recoil velocity.

B. Timing Accuracy

Precision measurements of the recoil frequency require precise measurements of the free evolution time in addition to precision measurements of phase evolution. In the process of investigating unexplained departures from linear phase evolution, questions arose about the accuracy of the quartz clock used as the time standard for the experiment's pulse sequences. The time to digital converter that was used to test the precision of the DDS was determined to be precise enough to test the experimental timing to the 0.5 ppb level (3 ps/6 ms), which is beyond the level of sensitivity needed to check whether timing issues were playing a role the current experiment, where

claimed levels of precision were at the 50 ppb level. Using the time to digital converter which was locked to a Cesium clock source, we tested the spacing between digital pulses triggered by the Cicero setup. This resulted in the discovery of two broad problems: first, the quartz clock used to define the length of experimental time steps had day-to-day fluctuations on the order of 1 part in 10^7 and a systematic offset of 1 part in 10^4. Second, many of the nominal times used had an additional 100 ns error which appeared to be due to a software issue in the Cicero word generator.

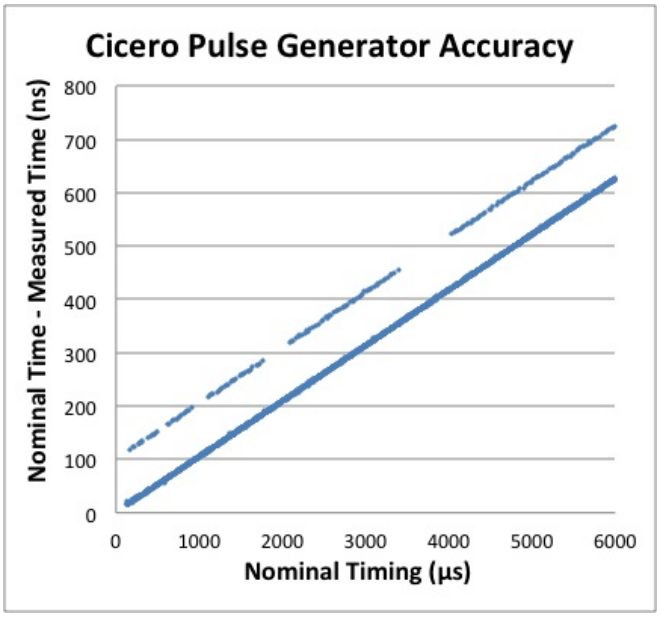

FIG. 7. Residual errors between nominal time and the time measured with the TDC. The points along the main line are shifted from zero due to the inaccuracy of the quartz clock. The points in the second line are offset by 100 ns (equal to a single clock cycle). Many of these points disappear when the units used to express timesteps in Cicero are changed from µs to ms.

1. *Switching to a Cesium Clock*

The results of the first check of the Cicero digital outputs against the time to digital converter showed a consistent offset of 1.0×10^{-4}. The slope of the line fit to the curve showed a total effect of errors in the quartz clock. Further tests showed that the slope of this line varied on a day-to-day basis at the level of 1×10^{-7}. Thus while prior data could be corrected up to this level, it would be impossible to correct up to the level of precision desired for the experiment in the long term. As a result, we decided to replace the quartz clock that had been used as a time base for the experiment with the same high precision cesium clock used as the time base for the TDC. Before the use of the Cesium clock, the difference between nominal time and actual measured time was at the 100 ppm level as is shown in Figure 7. After an output of the Cesium clock was used to replace the quartz clock, the disagreement between nominal time and measured time was reduced to essentially within the uncertainty of a flat relationship. This is seen in Figure 8. There is a remaining offset between nominal time and measured time, that is likely due to differences in the response to start and stop triggers on the TDC. More importantly, the slope is only 1.1 σ from zero, -12 ± 11 ppb. To the level of measurement accomplished with the TDC, the spacing between pulses is correctly controlled.

2. *Cicero Timing Glitches*

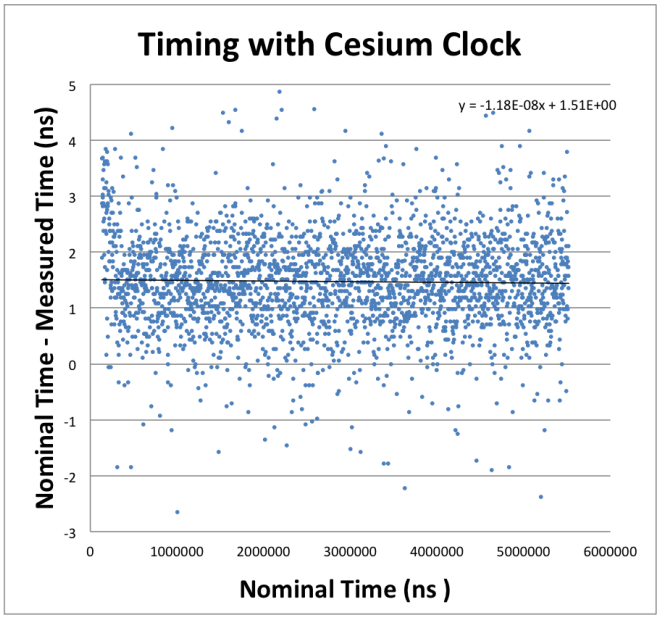

FIG. 8. Residual errors between nominal time and the time measured with the TDC after switching to Cesium Clock and removing the points with known glitches. There is an overall offset of 1.5 ns between the nominal times and actual measured times, but the slope is zero to within the standard error of the slope.

In addition to the errors due to the instability and systematic offset of the quartz clock, many apparently random values for nominal time were measured incorrectly by the timing software with an error of exactly 100 ns. Even after the overall error from the quartz clock was corrected, the pulse generator created, for example, a true spacing of 1001.9 µs between pulses when a nominal spacing of 1002 µs was put into the code. This occurred at reproducible times and was determined to be related to the units with which nominal times were input into the system (e.g. a nominal time of 1.002 ms accurately produced pulses spaced by 1002 µs).

These timing glitches proved difficult to predict from any first principle calculations (except for the pattern where problematic points were always multiples of 2

times other problematic points). However the problematic points proved to be reproducible, so we generated a list of points that were problematic. The list can be used to preemptively check whether there is a 100 ns offset at a given nominal time. Additionally, by switching the units from µs to ms, the total number of glitch points is reduced by a factor of three to 2%, making it less likely that these glitch points will be used in an experimental run. The problem seems to be a bug in the source code for Cicero, so we plan to report the error in the hopes that it can be corrected in future releases of the program. For the overall accuracy of the experiment, it appears to currently be sufficient to be aware of the problematic nominal times and exclude them from data collection runs.

V. CONCLUSIONS

Once technical challenges and systematic errors associated with transitioning to a vertical geometry are addressed, the long freefall times associated with a vertical diffraction geometry promise to make a sub-ppb level measurement of α possible using the Gupta Lab's contrast interferometry techniques. Switching to a vertical diffraction geometry allows for a dramatic increase in total phase accumulation to 12 million radians from the current value of approximately 120,000 radians. If the current 10 mrad absolute uncertainty is maintained this value is immediately competitive with the current 0.7 ppb accuracy in α from Rb recoil measurements. Modest further improvements in either absolute uncertainty or number of recoils puts 0.1 ppb accuracy within striking distance.

This summer progress was made towards preparing for technical challenges of a vertical diffraction geometry by setting up a new direct digital synthesizer (DDS) and designing RF paths capable of running vertical diffraction beams and compensating for gravity. Additionally, timing issues were resolved to better than 10 ppb, good enough for the current level of precision. However, additional tests will need to be made before asserting timing precision at the 0.1 ppb level.

The next step to implementing vertical diffraction in the experiment are redirecting the RF paths from the four digital synthesizers to match the design in figure 6 and then re-orienting the beams to a vertical orientation. This change risks damaging the current alignment of the apparatus and will not be attempted until current data taking runs are complete. However, once the changes are implemented we can hope to soon achieve sub-ppb level precision measurements of the fine structure constant.

VI. BIBLIOGRAPHY

[1] D. Hanneke, S. Fogwell, and G. Gabrielse, Phys. Rev. Lett. 100, 120801 (2008).
[2] T. Aoyama, M. Hayakawa, T. Kinoshita, and M. Nio, Phys. Rev. Lett. 109, 111807 (2012).
[3] R. Bouchendira, P. Clad, S. Guellati-Khlifa, F. Nez, and F. Biraben, Phys. Rev. Lett. 106, 080801 (2011)
[4] A. O. Jamison, B. Plotkin-Swing, and S. Gupta, Phys. Rev. A 90, 063606 (2014)
[5] P. J. Mohr, B. N. Taylor, and D. B. Newell, Rev. Mod. Phys. 80, 633 (2008); arXiv:1203.5425v1 (2012).
[6] R. Rana, M. Hocker, and E. G. Myers, Phys. Rev. A 86, 050502(R) (2012)
[7] A.O Jamison, Doctoral Thesis, University of Washington (2014)
[8] Wolfram, Alpha Knowledgebase, (2017)